

ATP-induced Reverse Temperature Effect in Isohemoglobins from the Endothermic Porbeagle Shark (*Lamna nasus*)*

Received for publication, February 24, 2003, and in revised form, May 6, 2003
Published, JBC Papers in Press, May 27, 2003, DOI 10.1074/jbc.M301930200

Christina Larsen, Hans Malte‡, and Roy E. Weber

From the Department of Zoophysiology, Institute of Biological Sciences, University of Aarhus, Building 131, 8000 Aarhus, Denmark

The evolutionary convergence of endothermic tunas and lamnid sharks is unique. Their heat exchanger-mediated endothermy represents an interesting example of the evolutionary pressure associated with this specific characteristic. To assess the implications of endothermy for gas transport and the possible contribution of hemoglobin (Hb), we investigated the effect of temperature on the oxygen equilibria of purified isohemoglobin components V and III from the porbeagle shark (*Lamna nasus*). In the absence of ATP the effect of temperature on oxygen affinity is normal in both Hb III ($P_{50} = 0.9$ and 2.2 torr at 10 and 26 °C, respectively) and Hb V ($P_{50} = 1.5$ and 2.5 torr at 10 and 26 °C, respectively). In the presence of this effector P_{50} decreases with increasing temperature in both components (P_{50} at 10 and 26 °C = 9.9 and 8.4 torr (Hb III), respectively, and 9.6 and 7.4 torr (Hb V), respectively). The reverse temperature effect in the presence of ATP will reduce the risk of oxygen loss from the arterial to the venous blood by lowering the oxygen tension gradient between the blood vessels. The mechanism behind the reverse temperature effect resembles that found in the bluefin tuna (*Thunnus thynnus*), an endothermic teleost, thus evidencing further convergent evolution.

True tunas and lamnid sharks are the only fish that have developed endothermy. The fact that this characteristic has evolved independently in two such different families (Scombridae and Lamnidae, respectively) makes these species choice subjects for comparison of the traits associated with endothermy (1–4). Endothermic fishes maintain body temperatures of up to 20 °C above ambient water temperatures, depending on species, water temperature, and activity level (5–7). The consequences of high core body temperatures for gas transport, ion balance, oxygen consumption, aerobic capacity, and muscle performance have been the subject of extensive studies in endothermic tuna species (for review, see Refs. 8–11); however, little is known about these relationships in elasmobranchs. The porbeagle shark (*Lamna nasus*) has a core body temperature of 8–10 °C above ambient water temperature (12) and has one of the highest body temperatures among the Lamnidae (13–15). As in tunas its endothermy is brought about by a number of countercurrent heat exchangers, *rete mirabilia*, placed in series with the heat-producing organ (16–18). The lateral heat exchangers are placed between the surroundings and the internally located red muscle, and the major blood supply to the red

muscle is directed through these via large cutaneous arteries and veins. By minimizing the heat loss via the blood, metabolically produced heat is retained within the active organ (5, 6).

One consequence of heat exchanger-mediated endothermy is that factors other than heat may be exchanged. The smaller the arteries and veins constituting the heat exchanger are, the more efficient the heat retention and the warmer the fish can be relative to the surrounding water. However, decreased dimensions of the heat exchanger increase the risk of oxygen diffusing from the cold arterial blood to the warm venous blood.

Already in 1960 Rossi-Fanelli and Antonini (19) showed that temperature has virtually no effect on oxygen binding of R-state crystalline Hb¹ from the endothermic bluefin tuna (*Thunnus thynnus*) at pH values between 6.45 and 8.7. Further studies revealed that although temperature does not influence P_{50} in the 10–30 °C temperature range, it does alter the shape of the oxygen equilibrium curve (20, 21), resulting from a normal temperature effect at low oxygen saturation and a reversed one at higher saturations.

The heat exchanger-mediated endothermy represents a curious incidence of convergent evolution. In this context it is interesting to investigate whether endothermy in the porbeagle shark is associated with adaptations in the temperature sensitivities of Hb, as documented in Hb I of bluefin tuna (19–21). This paper reports the effects of temperature, ATP, and pH on isolated Hb components III and V of the porbeagle shark. Previous studies on hemolysate indicate that the oxygen affinity of porbeagle shark blood is temperature-insensitive (22, 23); however, the allosteric mechanism behind the temperature effect remains to be investigated in purified isohemoglobins. Moreover the contribution of organic phosphates needs to be investigated in light of the observation that ATP induces a reverse temperature effect in striped marlin (*Tetrapturus audax*) Hb (24).

EXPERIMENTAL PROCEDURES

Heparinized blood from a porbeagle shark (*L. nasus*) was supplied from North Sea fishermen. Red blood cells were lysed by addition of three volumes of 0.1 M Tris buffer, pH 7.00 (25 °C). Following centrifugation for 15 min at 14,000 rpm to remove cell debris, the Hb stock solution was stored at –80 °C.

Preparation of Isohemoglobins and Oxygen Binding Studies—Isolation of the individual Hbs was performed using preparative isoelectric focusing (column, type 8102, Amersham Biosciences) at 3.9–4.5 °C (Fig. 1) after CO equilibration of the hemolysate. The ampholytes (Amersham Biosciences AB) used were pH 6–8 (40%) and pH 6.7–7.7 (60%) in a sucrose gradient. The seven separated components were dialyzed against three changes of CO-equilibrated, 10 mM Hepes buffer, pH 7.7, containing 0.5 mM EDTA.

Three Hb components (Hb V, IV, and III) accounted by far for most of the Hb (Fig. 1). Their isoelectric points at 16 °C were 7.58, 7.62, and

* This work was supported by the Oticon Foundation and the Danish Natural Science Research Council. The costs of publication of this article were defrayed in part by the payment of page charges. This article must therefore be hereby marked "advertisement" in accordance with 18 U.S.C. Section 1734 solely to indicate this fact.

‡ To whom correspondence should be addressed. Tel.: 45-89422596; Fax: 45-86194186; E-mail: Hans.Malte@biology.au.dk.

¹The abbreviations used are: Hb, hemoglobin; MWC, Monod-Wyman-Changeux.

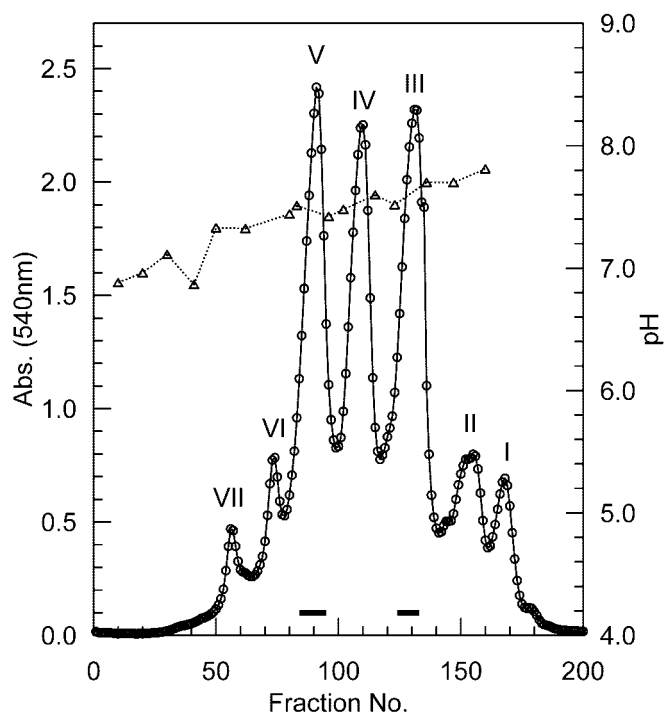


FIG. 1. Elution profile of porbeagle shark iso-hemoglobins isolated by preparative isoelectric focusing. Fractions V and III were chosen for study (see "Experimental Procedures"). The fractions pooled are indicated; pH was measured at 16 °C. Abs., absorbance.

7.68, respectively. Given the small differences in isoelectric points and the fact that fish Hbs with similar electrophoretic mobility exhibit basically similar functional properties (25), further investigations were focused on Hb V and III.

Hb concentrations were measured spectrophotometrically using millimolar extinction coefficients of oxyhemoglobin: 14.37 (β) and 15.37 (α) at 542 and 577 nm, respectively. Hb solutions were concentrated where necessary by ultrafiltration using Centrprep YM-10 tubes (Amicon Bioseparations, Millipore). Oxygen binding was measured at heme concentrations of 0.29–0.30 mM in 0.1 M Hepes buffer, pH 7.304 \pm 0.008. Values of pH were measured using a thermostatted BMS Mk2 capillary electrode (Radiometer, Copenhagen, Denmark) calibrated with S1500 and S1510 precision buffers (Radiometer).

Oxygen binding equilibria were generated at 10, 16, 21, and 26 °C in the absence or presence of ATP (ATP/Hb₄ ratio, >30) using a modified gas-diffusion chamber allowing stepwise increments of oxygen partial pressure (26). The chamber was coupled to two cascaded Wösthoff pumps (type M201a-f and M301) for admixture of atmospheric air, O₂, and pure N₂ (99.998%). Based on close similarity of the temperature sensitivities of Hbs III and V, analysis of the interactive effects of pH in the absence and presence of ATP was limited to Hb III.

Data Analysis—Extended Hill plots were analyzed using the MWC (two-state) model (27)

$$S = \frac{LK_T P(1 + K_T P)^{(q-1)} + K_R P(1 + K_R P)^{(q-1)}}{L(1 + K_T P)^q + (1 + K_R P)^q} \quad (\text{Eq. 1})$$

where S denotes saturation, P the partial pressure of oxygen, L the allosteric constant, K_T and K_R the association constants for the low affinity (T, tense) and the high affinity (R, relaxed) forms, respectively, and q the number of interacting binding sites. Based on the results of Andersen *et al.* (23), who performed ultracentrifugation on hemolysate of porbeagle shark blood and found the slope of the absorbance *versus* radius squared to be consistent with a homogenous solution of tetrameric hemoglobins, the Hb was assumed tetrameric, and a fixed value of $q = 4$ was imposed at all times. Non-linear least squares curve fitting was performed using the software package Mathematica® (Wolfram Research Inc., Cambridge, MA) employing the Levenberg-Marquardt method. Estimates of the standard errors of the fitted parameters were obtained from the diagonal elements of the curvature matrix associated with the fit (26). To minimize the errors introduced by incomplete saturation or desaturation, when equilibrating with pure oxygen or nitrogen, respectively, the absorbance values at zero and full

saturation were extrapolated from the data in the fitting procedure as described by Fago *et al.* (26).

P_{50} , the oxygen tension at half-saturation of the Hb, was calculated as the PO_2 value at $\log(S/(1 - S)) = 0$, and n_{50} was calculated as $\partial \log(S/(1 - S))/\partial \log PO_2$ at that PO_2 . The median oxygen tension P_m was calculated from

$$P_m = (1/K_R)[(L + 1)/(Lc^q + 1)]^{(1/q)} \quad (\text{Eq. 2})$$

where $c = K_T/K_R$ (28, 29).

The free energy of heme-heme interaction ΔG was calculated according to Wyman *et al.* (30).

$$\Delta G = RT \ln \frac{(L + 1)(Lc^q + 1)}{(Lc + 1)(Lc^{q-1} + 1)} \quad (\text{Eq. 3})$$

The difference in bond energies in the R and T states between the absence and presence of ATP was calculated as $\Delta G = RT \ln(K_{x,ATP}/K_x)$, where x denotes the T or R state.

The heat of oxygenation was calculated according to the following relationship

$$\Delta H = 2.303 \times R \times \Delta \log X \left(\frac{1}{T_1} - \frac{1}{T_2} \right) \quad (\text{Eq. 4})$$

where R is the gas constant, X is P_{50} , $1/L$, $1/K_T$, or $1/K_R$, and T is the absolute temperature. ΔH_{app} is ΔH at P_{50} and includes the heat of release of effectors and solution of ligands and the heat of oxygen binding.

RESULTS

Effects of Temperature and ATP—Extended Hill plots of the oxygen equilibria of Hbs III and V at pH 7.3 and at four temperatures (10, 16, 21, and 26 °C) each in the presence or absence of ATP are shown (Fig. 2). The MWC model was successfully fitted to the data. In all instances P_{50} of the fitted curves was similar to P_m , and the fitted curves were symmetrical around P_{50} .

Both Hbs exhibit high intrinsic oxygen affinities (low P_{50} values) (Table I) and small, normal temperature effects at half-saturation ($\Delta H = -40.1$ and -20.7 kJ·mol⁻¹ in Hbs III and V, respectively) at pH 7.3 (Table II). Increasing temperature from 10 to 26 °C increases P_{50} from 0.9 to 2.2 torr (Hb III) and from 1.5 to 2.5 torr (Hb V) (Table I). The addition of ATP reduces the oxygen affinity in Hbs III and V, but less so at higher temperatures, resulting in a small reverse temperature effect in both Hbs ($\Delta H = 12.2$ and 11.6 kJ·mol⁻¹ in Hbs III and V, respectively) (Table II).

Fig. 3 shows the temperature dependence of P_{50} (the van't Hoff plot) and n_{50} with and without ATP present. A reverse temperature effect in the presence of ATP is seen. ATP additionally increases cooperativity expressed as n_{50} (Fig. 3, lower panel), particularly at high temperature. As evident, Hb III and V show very similar oxygenation characteristics.

Mechanisms of the Temperature Effect—The MWC parameters L , K_R , and K_T provide a mechanistic basis for the effects of temperature on the Hbs (Fig. 4 and Table I). At increasing temperature L decreases, indicating a destabilization of the T (tense) state relative to the R (relaxed) state (Fig. 4a). ATP stabilizes the T state (increases L) but only slightly affects the temperature sensitivity.

Increasing temperature decreases oxygen affinity of the R and T states in Hb III and V, but more so in the R state (Fig. 4, b and c). ATP reduces the oxygen affinities of both the T and R states and their temperature sensitivities, making K_T of both Hbs insensitive to temperature change, whereas K_R is still somewhat reduced by increasing temperature. The effect of ATP on K_R decreases with increasing temperatures, indicating that ATP also binds to the R state, particularly at low temperatures. The T state becomes less stable at high temperatures (L decreases), and the overall oxygen binding to the T state accordingly decreases.

FIG. 2. Hill plots of oxygen equilibria of porbeagle shark at pH 7.3. a, Hb V. b, Hb III. Lines represent the fitting of the MWC model to the data. Diamonds, at 10 °C; squares, at 16 °C; circles, at 21 °C; triangles, at 26 °C; open symbols, in the absence of ATP; filled symbols, in the presence of ATP.

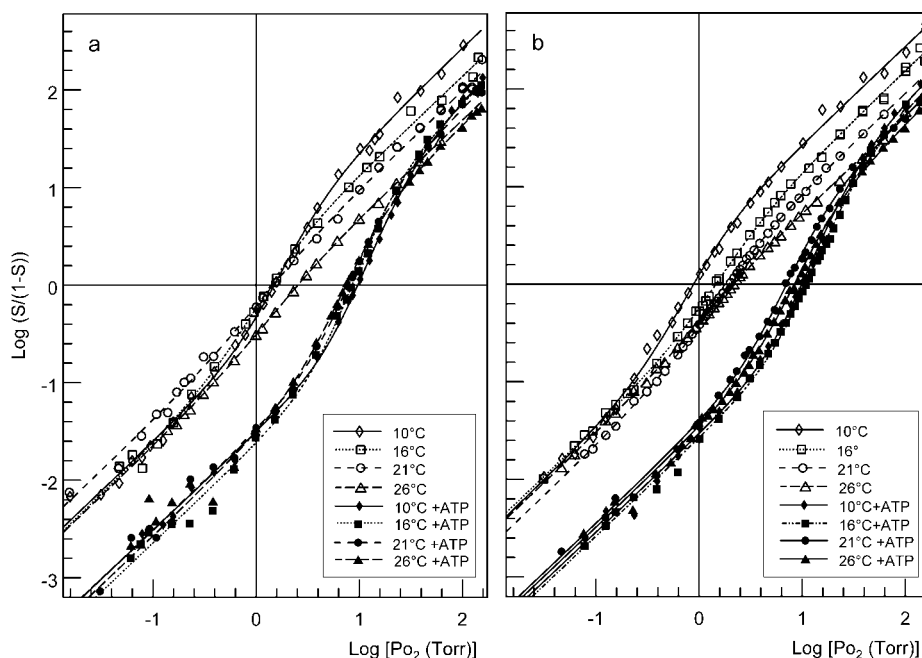


TABLE I
MWC and derived parameters for Hb V and III

Hb sample	Temperature °C	P_{50} torr	n_{50}	n_{max}	P_m torr	Log L	S.E. ^a	Log K_T	S.E. ^a	Log K_R	S.E. ^a	ΔG kJ·(mol of heme) ⁻¹
V	10	1.50	1.93	1.94	1.44	2.66	0.219	-0.622	0.0417	0.505	0.0561	1.42
	16	1.39	1.63	1.66	1.47	1.25	0.271	-0.814	0.300	0.150	0.0699	1.10
	21	1.46	1.28	1.28	1.50	0.725	0.362	-0.570	0.165	0.0211	0.0745	0.562
	26	2.54	1.22	1.26	2.68	0.330	0.0994	-1.075	0.183	-0.304	0.0215	0.513
V + ATP	10	9.65	2.34	2.38	9.04	3.95	0.219	-1.514	0.0272	0.0313	0.0790	1.98
	16	8.52	2.52	2.53	8.39	3.33	0.271	-1.65	0.0426	-0.0907	0.0636	2.12
	21	7.81	2.30	2.30	7.66	3.00	0.362	-1.52	0.0319	-0.134	0.0510	1.89
	26	7.44	2.14	2.15	7.70	2.18	0.0994	-1.62	0.0710	-0.340	0.0448	1.76
III	10	0.883	1.82	1.84	0.923	1.65	0.148	-0.614	0.0939	0.446	0.0376	1.30
	16	1.45	1.53	1.53	1.44	1.69	0.128	-0.516	0.0285	0.263	0.0321	0.920
	21	1.94	1.48	1.49	2.02	1.10	0.0462	-0.809	0.0283	-0.0225	0.0126	0.884
	26	2.16	1.16	1.19	2.27	0.093	0.0791	-1.05	0.188	-0.268	0.0135	0.384
III + ATP	10	9.89	2.36	2.39	9.33	3.84	0.299	-1.54	0.0292	-0.0106	0.0757	1.98
	16	10.9	2.33	2.36	10.34	3.70	0.334	-1.59	0.0266	-0.0910	0.0868	1.98
	21	7.06	2.13	2.13	7.07	2.47	0.150	-1.48	0.0327	-0.232	0.0395	1.69
	26	8.38	2.08	2.08	8.35	2.44	0.161	-1.51	0.0249	-0.311	0.0434	1.65

^a Standard error of the fitted parameters.

TABLE II
The apparent heat of reaction, ΔH_{app} , for L, the T and R states, and at half-saturation oxygen tension (P_{50}) in Hb III and V in the absence or presence of ATP

Hb sample	ΔH			P_{50}
	L	T	R	
	$\text{kJ}\cdot\text{mol}^{-1}$			
V	-222	-27.1	-81.5	-20.7
V + ATP	-182	-4.97	-38.0	11.6
III	-184	-66.6	-77.8	-40.1
III + ATP	-152	5.51	-31.5	12.2

The reverse temperature effect in the presence of ATP thus stems from the combined effects of the reduction of L with increasing temperature and reduced temperature sensitivity of the T state and especially of the R state. These effects are reflected by the temperature invariance of the lower asymptotes of the extended Hill plots in Fig. 2 (constant K_T values) and a change in the slope of the curve around $\log[S/(1-S)] = 0$ as L falls at higher temperatures. The change in K_R is evident

from the greater stability of the upper asymptotes of the curves in the presence of ATP than in its absence.

Free Energies and Enthalpies of Reaction—In the absence of ATP the free energy of heme-heme interaction, ΔG , falls with increasing temperature (Table I). By stabilizing the T state, as evidenced by the temperature invariance of K_T and the increase in L (Fig. 4), ATP increases the free energy of cooperativity but does so more at high than at low temperature, thus resulting in a low ATP sensitivity at high temperature. The change in ΔG mirrors the effect of temperature on L and n_{50} and reflects the ATP-induced increased cooperativity.

In both Hb III and V, ATP increases the apparent (overall) heat of oxygenation, ΔH_{app} (ΔH at P_{50}), which becomes positive (Table II). This effect is consistent with the elevation of ΔH_L , ΔH_T , and ΔH_R by ATP (Table II).

The displacement of the lower asymptote of the Hill plots in the presence of ATP reflects the additional bond energies that stabilize the T state in the presence of the polyanionic phosphate anion (Fig. 2). The ATP-induced bond energy differences are greater in the T state than in the R state (4.8–5.0 kJ·mol

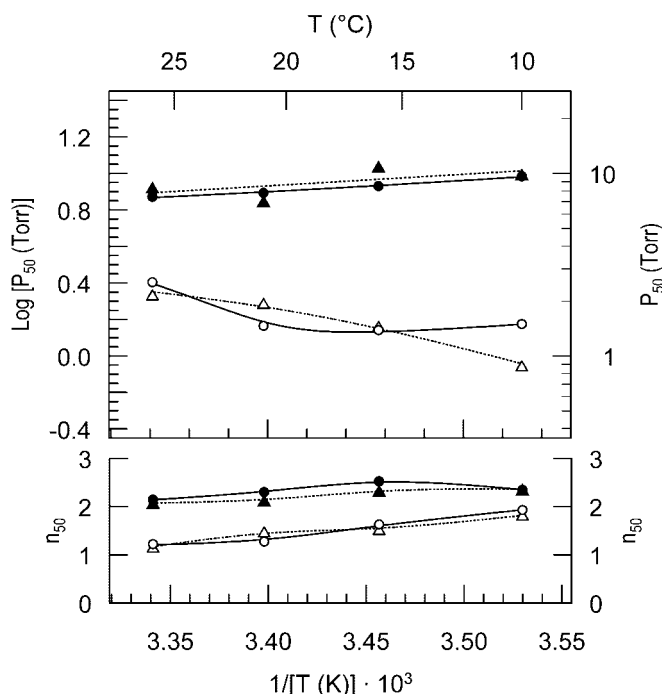


FIG. 3. The effect of different temperatures on P_{50} (van't Hoff plots) and n_{50} for Hb III (.....) and V (—) at pH 7.3 in the absence (open symbols) or presence (filled symbols) of ATP.

of heme)⁻¹ compared with 2.5–2.6 kJ·(mol of heme)⁻¹ for both Hbs at 10 °C and pH 7.3; Table III). Additionally, the bond energy difference decreases with increasing temperature in both the T and R states. The difference in bond energy, ΔG_T and ΔG_R , with and without ATP is presented in Table III.

Effect of Changes in pH—Hill plots of oxygen equilibria of Hb III at 10 and 26 °C with and without ATP and at different pH values were fitted using the MWC model (Figs. 5 and 6). The pH sensitivities of P_{50} and n_{50} are shown in Fig. 7. At 10 °C Hb III shows a reverse Bohr effect between pH 8.3 and 7.5 ($\varphi \sim 0.5$) that becomes normal at pH < 7.5 ($\varphi \sim -0.6$). At 26 °C the phosphate-free Hb show no Bohr effect in the experimental range of pH values. In the presence of ATP the Bohr effect becomes normal at both temperatures. Noticeably, the reverse temperature dependence with ATP present is marked at low pH and phases out at high pH (Fig. 7). The Bohr effect at pH ~ 7.0 –7.3 in the presence of ATP is larger at 10 °C ($\varphi \sim -0.76$) than at 26 °C ($\varphi \sim -0.3$).

The cooperativity coefficient n_{50} is negatively affected by lowering pH at low temperature, whereas it is positively affected at high temperature (Fig. 7) and invariably higher in the presence of ATP than in phosphate-free solution. The n_{50} values at 10 °C exceed those at 26 °C at all pH values when ATP is absent and above pH 7.3 with ATP.

Mechanisms of the Bohr Effect—The allosteric control mechanisms of the Bohr effect are illustrated in Fig. 8. At 10 °C without ATP L decreases from $>10^4$ at pH 8.0 to $\sim 10^2$ at a pH of 7.6, indicating a destabilization of the T state at low pH. The reverse Bohr effect at 10 °C in the absence of ATP described previously concurs with the large fall in L as pH is lowered, whereas K_T and K_R remain unchanged (Fig. 8). With ATP present this effect is shifted to a lower pH (6.7); the pH effect becomes normal, K_T decreases, and K_R drops drastically as pH falls below 7.5. At 26 °C the effect of pH on L , K_T , and K_R is negligible in the absence of ATP. At 26 °C ATP elevates L by stabilizing the T state, in part because of a stabilizing effect of additional proton binding to the T state, its effect being larger at low pH. Concurrently, K_T becomes lower and slightly de-

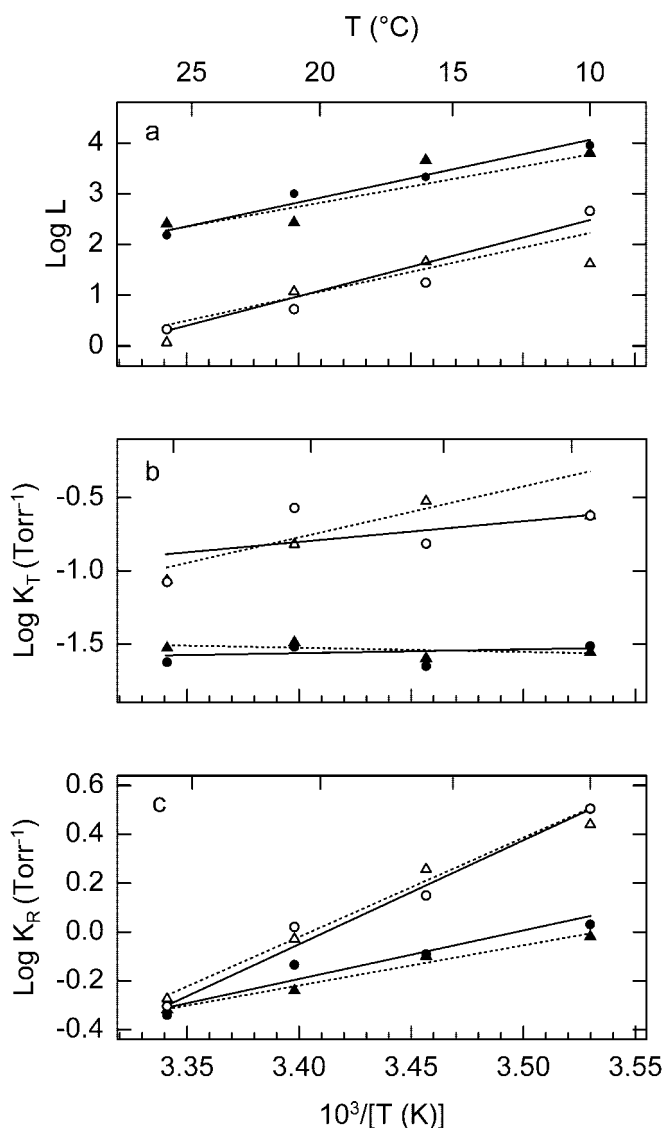


FIG. 4. Temperature dependence of the allosteric parameters of the MWC model for Hb III (triangles,) and V (circles, —) in the absence (open symbols) or presence (filled symbols) of ATP. a, the allosteric constant, L . b, the association constant for the T state, K_T . c, the association constant for the R state, K_R . Linear regressions are fitted to the weighted data points presented in Table I.

TABLE III
The differences in bond energies of Hb III and V in the T or R state in the presence compared to the absence of ATP

Hb	Temperature °C	ΔG	
		ΔG_T kJ·(mol of heme) ⁻¹	ΔG_R kJ·(mol of heme) ⁻¹
V	10	4.83	2.57
	16	4.63	1.33
	21	5.34	0.875
	26	3.15	0.210
III	10	5.04	2.48
	16	5.92	1.96
	21	3.76	1.18
	26	2.64	0.245

creases at lower pH values, and K_R remains low and stable irrespective of the presence ATP (Fig. 8).

Free Energies of Reaction—The free energy of heme-heme interaction (ΔG) is slightly higher at 10 °C than at 26 °C over the entire pH range and in the presence of ATP than in stripped Hb (Table IV). In the absence of ATP, ΔG varies only

FIG. 5. Hill plots for oxygen equilibrium of porbeagle shark Hb III at different pH values. *a*, at 10 °C. *b*, at 26 °C. Lines represent the fitting of the MWC model to the data.

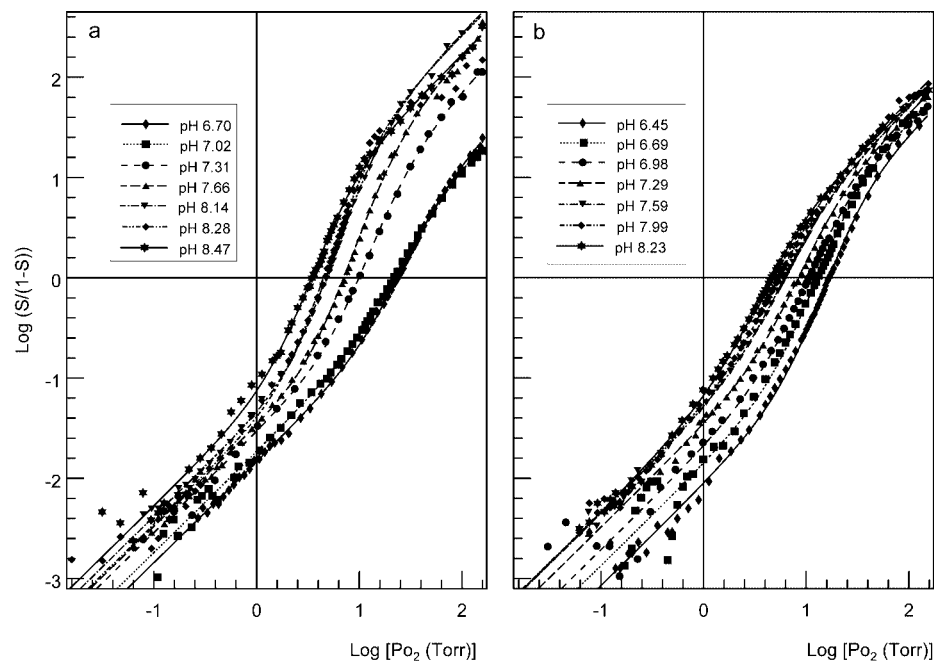
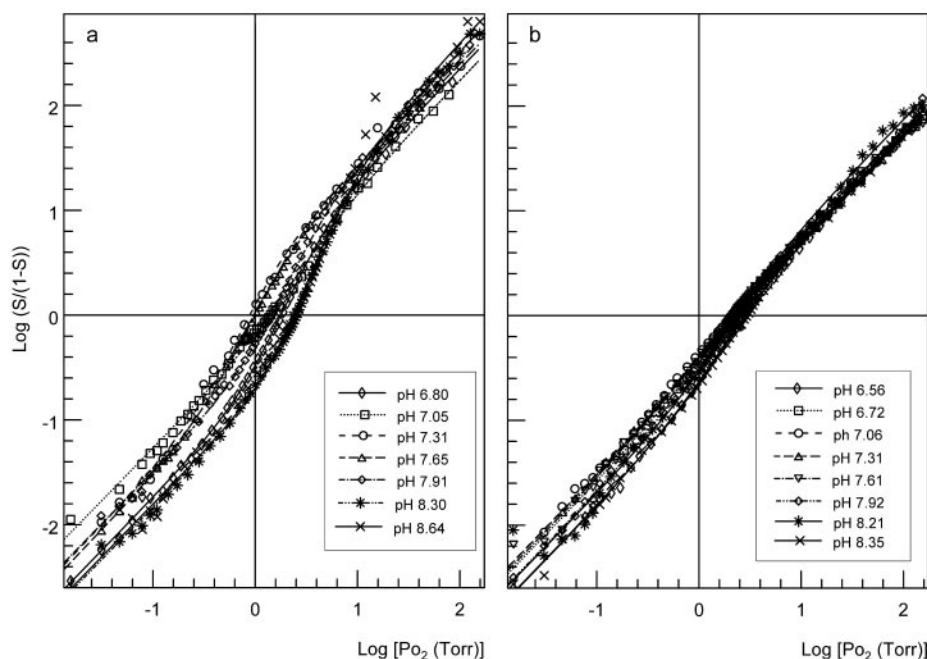


FIG. 6. Hill plots for oxygen equilibrium of Hb III with ATP (ATP/Hb >30) at different pH values. *a*, at 10 °C. *b*, at 26 °C. Lines represent the fitting of the MWC model to the data.

slightly with pH. With ATP ΔG decreases at low pH (<7.5 at 10 °C) and increases at high pH (>7.0 at 26 °C) (Table IV).

DISCUSSION

The MWC model, which assumes functional homogeneity between the subunits comprising the tetrameric Hb, successfully describes the oxygen binding characteristics of porbeagle shark Hb. This indicates either that the chain heterogeneity found in porbeagle shark hemolysate (23) is not found in the purified Hb components investigated in this study or that it does not influence oxygen binding.

The reverse temperature effect on isolated Hb III and V from porbeagle shark resembles that in bluefin tuna Hb I in phosphate buffer (21). In Hbs from both species low temperature stabilizes the T state, and a reverse temperature effect on K_R is seen at low pH. The difference between the two species is qualitative. In the bluefin tuna the stabilization of the T state at low temperature (high L) abolishes the T \rightarrow R transition.

Therefore, oxygen binds in the T state even at high oxygen saturation levels, revealing the presence of two functionally distinct subunits in the T state (21). In porbeagle shark the T \rightarrow R transition does occur, and we find no evidence for differences in the two subunits comprising the Hb. Our results thus agree with those of Andersen and co-workers (23), who found a reverse temperature effect in hemolysate in the 5–15 °C range and a decrease in L with rising temperature. Thus it appears that the evolutionary convergence of endothermic tunas and lamnid sharks includes changes in the functional mechanisms of their main Hb components.

In porbeagle shark Hb the reverse temperature effect is only seen at pH values below 7.5 and in the presence of ATP (Fig. 7). We find that the reverse temperature effect is caused largely by an increase in the allosteric constant, L , with decreasing temperature (Fig. 4). Although acting in the opposite direction, the concurrent increase in K_R at pH 7.3 in the presence of ATP is

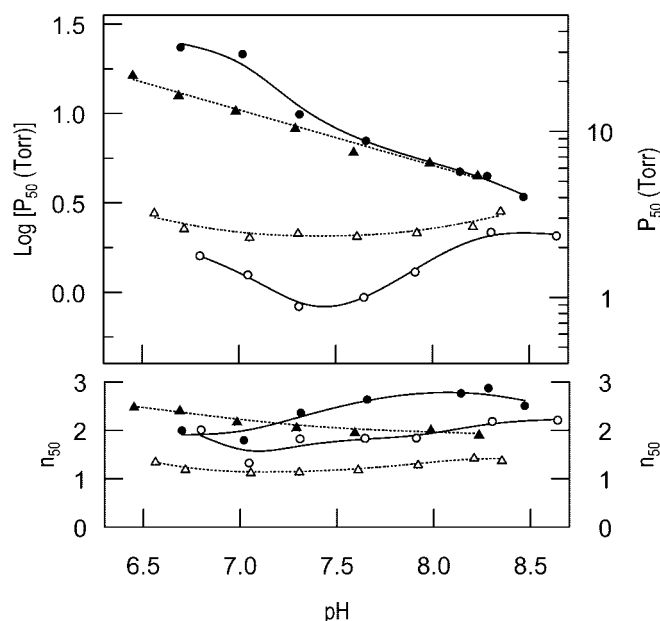


FIG. 7. The effect of pH on P_{50} and n_{50} of Hb III at 10 (circles, —) and 26 °C (triangles,) in the absence (open symbols) or presence (filled symbols) of ATP.

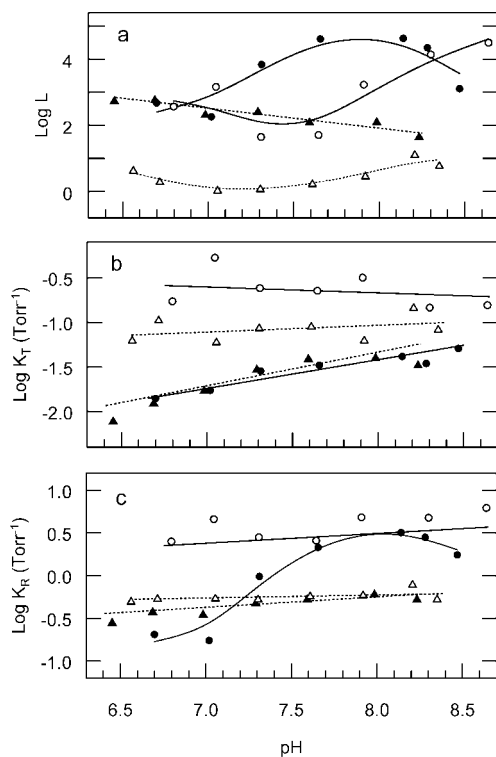


FIG. 8. The parameters of the MWC model for Hb III at 10 (circles, —) and 26 °C (triangles,) at different pH values in the absence (open symbols) or presence (filled symbols) of ATP. a, L . b, K_T . c, K_R .

insufficient to counteract the effect of L . At lower pH values the temperature effect on K_R becomes reversed, and this magnifies the overall reverse temperature effect. The effect of ATP on K_R is most prominent at low pH, where it increases the magnitude of the reverse temperature effect, and more or less vanishes at pH values ≥ 7.7 (Fig. 8). The lack of an effect of ATP at 26 °C indicates that no ATP is allosterically bound to the oxyhemoglobin at this temperature. The bond energy per salt bridge is

TABLE IV

The free energy of heme-heme interaction for Hb III and V at different pH values, at 10 and 26 °C, and in the presence and absence of ATP

Temperature	No ATP		ATP	
	pH	ΔG	pH	ΔG
°C		$\text{kJ} \cdot (\text{mol of heme})^{-1}$		$\text{kJ} \cdot (\text{mol of heme})^{-1}$
10	6.798	1.49	6.699	1.49
	7.046	0.70	7.019	1.24
	7.309	1.30	7.313	1.98
	7.645	1.30	7.656	2.37
	7.910	1.38	8.141	2.5
	8.302	1.85	8.282	2.6
	8.640	1.93	8.470	2.05
26	6.563	0.77	6.452	2.19
	6.717	0.47	6.689	2.08
	7.055	0.37	6.984	1.81
	7.305	0.38	7.291	1.65
	7.610	0.48	7.593	1.53
	7.919	0.69	7.986	1.60
	8.208	0.84	8.234	1.55
	8.352	0.79		

4–8 $\text{kJ} \cdot \text{mol}^{-1}$ (31), which suggests that an additional salt bridge per heme group constrains the T state when ATP is present (Table III). The small changes in the differential bond energy in the R state further indicate the preferential binding of ATP to the T state relative to the R state, although additional weaker bonds may be implicated, particularly at high temperature, where the difference bond energy is below 4 $\text{kJ} \cdot \text{mol}^{-1}$.

At pH 7.3 (which likely falls in the physiological intraerythrocytic range) the overall ΔH_{app} is negative (oxygenation is exothermic) in the absence of ATP but becomes positive (oxygenation is endothermic) with ATP (Table II). The increase is due to the positive heat of ATP and proton release from the Hb during the T \rightarrow R transition. The fact that ΔH_T is much less negative (or positive) than ΔH_R is due to a greater ATP and proton release in the T state. Thus the addition of ATP obliterates the temperature effect in the T state, whereas it persists in the R state at high pH and is reversed at pH below 7.3 (Figs. 2, 4, and 7 and Table I). In bluefin tuna the temperature effect is normal in the T state (ΔH_1 is $-8.0 \text{ kJ} \cdot \text{mol}^{-1}$, and ΔH_2 is $-11.0 \text{ kJ} \cdot \text{mol}^{-1}$) and reversed in the R state (ΔH_3 and ΔH_4 are 10.4 and 21.3 $\text{kJ} \cdot \text{mol}^{-1}$, respectively) at pH 7.0 (21). In contrast, in trout Hb I, the effect of temperature on CO binding shows opposite dependence on ligand saturation; ΔH_T is 6 $\text{kJ} \cdot \text{mol}^{-1}$, and ΔH_R is $-11.3 \text{ kJ} \cdot \text{mol}^{-1}$ (21, 30). In tench (*Tinca tinca*) the addition of ATP increases ΔH_T (-55.8 to $-30.9 \text{ kJ} \cdot \text{mol}^{-1}$) and slightly decreases ΔH_R (-60.5 to $-68.0 \text{ kJ} \cdot \text{mol}^{-1}$) at pH 7.35, indicating that the proton release occurs gradually and that ATP does not bind to the R state (32).

Our results illustrate the complex relationship between pH and ΔH_{app} (Fig. 7). In the presence of ATP at pH values below 7.7, ΔH_{app} becomes increasingly positive with falling pH because of an increasing ΔH_L that eventually becomes positive at pH < 6.7 and an increasing ΔH_R that becomes positive at pH < 7.1 (Fig. 8, a and c). In spiny dogfish (*Squalus acanthias*), the ΔH_{app} of stripped Hb also is pH-dependent with a value of $-35 \text{ kJ} \cdot \text{mol}^{-1}$ at pH 7.0 and $-44 \text{ kJ} \cdot \text{mol}^{-1}$ at pH 7.9 (33).

The free energies of cooperativity, ΔG , at 10 and 26 °C with ATP (Hb III) are comparable to those found in tench (6.1 $\text{kJ} \cdot (\text{mol of Hb})^{-1}$) (34). Human Hb has a higher ΔG at 25 °C (8.8 $\text{kJ} \cdot (\text{mol of Hb})^{-1}$ at pH 7.4), close to values found at 10 °C with ATP at high pH (Hb III, Table IV) and at 16 °C with ATP (Hb V, Table I) (35).

The Bohr effect in porbeagle shark Hb at 10 °C with ATP ($\varphi \sim -0.76$) is large and similar to values for other active fishes. Albacore tuna (*Thunnus alalunga*) and striped marlin

have Bohr factors of -1.2 and -1.0 , respectively (36, 37), whereas those obtained from the moderately active blue shark (*Prionace glauca*) stripped hemoglobin with and without added inositol hexaphosphate are -1 and -0.4 , respectively (38). It is notable that the reverse Bohr effect at low temperature and in the absence of ATP extends to high pH values (7.5–8.3). The reverse Bohr effect is seen in other fish Hbs but is usually restricted to cathodic Hbs (for review, see Ref. 39), where it also disappears when ATP is present. This suggests that upon oxygenation alkaline Bohr groups change pK value in the reverse direction from normal.

Possible Implications for Oxygen Transport—Allosteric cofactors such as organic phosphates and protons lower the intrinsically high oxygen affinity of Hb to values that ensure oxygen unloading at oxygen tensions that are sufficiently high for physiological needs. Compared with small Bohr effects reported in sluggish elasmobranch species (40), active ones, like the porbeagle and mako sharks, have substantial Bohr effects at low temperature and in the presence of ATP (23). The pH insensitivity on K_R has been interpreted as advantageous under changing environmental oxygen tensions (34). By maintaining a constant high affinity for oxygen in the R state, loading is protected during hypoxia and during exercise when the blood may become acidotic. In porbeagle shark K_R falls at low temperature when pH is low, an effect not present at high temperature when environmental, dissolved oxygen concentration can be assumed to be lower and loading may become compromised.

The concentration of ATP and other organic phosphates in nucleated fish red cells decreases under conditions of decreased oxygen availability, forming a regulatory mechanism that favors oxygen loading through the resulting increase in oxygen affinity. During exercise the affinity gain may, however, be offset by the decreased blood pH (Bohr effect). In elasmobranchs the presence of high urea levels may hinder oxygen affinity modulation by dampening the ATP effect as seen in stripped hemolysate of spiny dogfish (33).

The presence of countercurrent heat exchangers in the porbeagle shark imposes a risk of oxygen loss from the arterial to the venous blood. However, as in the endothermic bluefin tuna, the presence of a reverse temperature effect in isolated Hb indicates that this risk is reduced. The increased oxygen affinity with rising temperature reduces the oxygen tension gradient between the arterial and venous blood. This adaptation to an efficient heat conservation mediated by heat exchangers may only be necessary in cases in which the heat exchangers are very efficient. As such the bluefin tuna and the porbeagle shark are the among the warmest species in their distantly related families, respectively, each representing very efficient countercurrent heat exchangers (6, 13–16, 41–43).

Acknowledgments—We extend thanks to an anonymous reviewer for helpful comments on the manuscript and to A. Bang for technical assistance.

REFERENCES

- Block, B. A., and Finnerty, J. R. (1994) *Environ. Biol. Fishes* **40**, 283–302
- Block, B. A., Finnerty, J. R., Stewart, A. F. R., and Kidd, J. (1993) *Science* **260**, 210–213
- Graham, J. B., and Dickson, K. A. (2000) *Zool. J. Linn. Soc.* **129**, 419–466
- Bernal, D., Dickson, K. A., Shadwick, R. E., and Graham, J. B. (2001) *Comp. Biochem. Physiol. Part A Mol. Integr. Physiol.* **129**, 695–726
- Carey, F. G., and Teal, J. M. (1969) *Comp. Biochem. Physiol.* **28**, 205–213
- Carey, F. G., Teal, J. M., Kanwisher, J. W., and Lawson, K. D. (1971) *Am. Zool.* **11**, 137–145
- Dewar, H., Graham, J. B., and Brill, R. W. (1994) *J. Exp. Biol.* **192**, 33–44
- Jones, D. R., Brill, R. W., and Mense, D. C. (1986) *J. Exp. Biol.* **120**, 201–213
- Dewar, H., and Graham, J. (1994) *J. Exp. Biol.* **192**, 13–31
- Dickson, K. A. (1995) *Environ. Biol. Fishes* **42**, 65–97
- Altringham, J. D., and Block, B. A. (1997) *J. Exp. Biol.* **200**, 2617–2627
- Carey, F. G., and Teal, J. M. (1969) *Comp. Biochem. Physiol.* **28**, 199–204
- Goldman, K. J. (1997) *J. Comp. Physiol. Biochem. Syst. Environ. Physiol.* **167**, 423–429
- Carey, F. G., Teal, J. M., and Kanwisher, J. W. (1981) *Physiol. Zool.* **54**, 334–344
- Anderson, S. D., and Goldman, K. J. (2001) *Copeia* **3**, 794–796
- Carey, F. G. (1973) *Sci. Am.* **228**, 36–44
- Graham, J. B. (1975) *Fish. Bull. (Wash. D. C.)* **73**, 219–229
- Burne, R. H. (1923) *Philos. Trans. R. Soc. Lond.-Biol. Sci.* **212B**, 209–257
- Rossi-Fanelli, A., and Antonini, E. (1960) *Nature* **186**, 895–896
- Carey, G. F., and Gibson, Q. H. (1977) *Biochem. Biophys. Res. Commun.* **78**, 1376–1382
- Ikedo-Saito, M., Yonetani, T., and Gibson, Q. H. (1983) *J. Mol. Biol.* **168**, 673–686
- Hazard, E. S., and Gibson, Q. H. (1984) *Am. Soc. Zool.* **24**, A120 (abstr.)
- Andersen, M. E., Olson, J. S., Gibson, Q. H., and Carey, F. G. (1973) *J. Biol. Chem.* **248**, 331–341
- Weber, R. E., and Jensen, F. B. (1988) *Annu. Rev. Physiol.* **50**, 161–179
- Weber, R. E. (2000) in *Hemoglobin Functions in Vertebrates: Molecular Adaptations to Extreme and Temperate Environments* (di Prisco, G., Giardina, B., and Weber, R. E., eds) pp. 23–27, Springer-Verlag, Milan, Italy
- Fago, A., Bendixen, E., Malte, H., and Weber, R. E. (1997) *J. Biol. Chem.* **272**, 15628–15635
- Monod, J., Wyman, J., and Changeaux, J.-P. (1965) *J. Mol. Biol.* **12**, 88–118
- Imai, K. (1982) *Allosteric Effects in Haemoglobin*, Cambridge University Press, Cambridge, UK
- Weber, R. E., Malte, H., Braswell, E. H., Oliver, R. W. A., Green, B. N., Sharma, P. K., Kuchumo, A., and Vinogradov, S. N. (1995) *J. Mol. Biol.* **251**, 703–720
- Wyman, J., Gill, S. J., Noll, L., Giardina, B., Colosimo, A., and Brunori, M. (1977) *J. Mol. Biol.* **109**, 195–205
- Perutz, M. F. (1970) *Nature* **228**, 726–739
- Jensen, F. B., and Weber, R. E. (1987) *J. Comp. Physiol. Biochem. Syst. Environ. Physiol.* **157**, 137–143
- Weber, R. E., Wells, R. M. G., and Rossetti, J. E. (1983) *J. Exp. Biol.* **103**, 109–120
- Weber, R. E., Jensen, F. B., and Cox, R. P. (1987) *J. Comp. Physiol. Biochem. Syst. Environ. Physiol.* **157**, 145–152
- Imai, K. (1973) *Biochemistry* **12**, 798–808
- Cech, J. J., Laurs, R. M., and Graham, J. B. (1984) *J. Exp. Biol.* **109**, 21–34
- Dobson, G. P., Wood, S. C., Daxboeck, C., and Perry, S. F. (1986) *Physiol. Zool.* **59**, 150–156
- Pennelly, R. P., Noble, R. W., and Riggs, A. (1975) *Comp. Biochem. Physiol.* **52B**, 83–87
- Fago, A., Carratore, V., di Prisco, G., Feuerlein, R. J., Sottrup-Jensen, L., and Weber, R. E. (1995) *J. Biol. Chem.* **270**, 18897–18902
- Wells, R. M. G., and Weber, R. E. (1983) *J. Exp. Biol.* **103**, 95–108
- McCosker, J. E. (1987) *Copeia* **1**, 195–197
- Holland, K. N., and Sibert, J. R. (1994) *Environ. Biol. Fishes* **40**, 319–327
- Carey, F. G., Kanwisher, J. W., Brazier, O., Gabrielson, G., Casey, J. G., and Pratt, H. L. (1982) *Copeia* **2**, 254–260